MISSOURI S&T

Missouri University of Science and Technology

Scholars' Mine

Electrical and Computer Engineering Faculty Research & Creative Works

Electrical and Computer Engineering

01 Jan 2006

Design of Optimal PI Controllers for Doubly Fed Induction Generators Driven by Wind Turbines using Particle Swarm Optimization

Wei Qiao

Ganesh K. Venayagamoorthy
Missouri University of Science and Technology

Ronald G. Harley

Follow this and additional works at: https://scholarsmine.mst.edu/ele_comeng_facwork

Part of the Electrical and Computer Engineering Commons

Design of Optimal PI Controllers for Doubly Fed Induction Generators Driven by Wind Turbines Using Particle Swarm Optimization

Wei Qiao, *Student Member, IEEE*, Ganesh K. Venayagamoorthy, *Senior Member, IEEE*,
and Ronald G. Harley, *Fellow, IEEE*

Abstract – **When subjected to transient disturbances in the power grid, the variable frequency converter (VFC) is the most sensitive part in the variable-speed wind turbine generator system (WTGS) equipped with a doubly fed induction generator (DFIG). The VFC is normally controlled by a set of PI controllers. Tuning these PI controllers is a tedious work and it is difficult to tune the PI gains optimally due to the nonlinearity and the high complexity of the system. This paper presents an approach to use the particle swarm optimization algorithm to design the optimal PI controllers for the rotor-side converter of the DFIG. A new time-domain fitness function is defined to measure the performance of the controllers. Simulation results show that the proposed design approach is efficient to find the optimal parameters of the PI controllers and therefore improves the transient performance of the WTGS over a wide range of operating conditions.**

I. INTRODCUTION

The worldwide concern about the environmental pollution and the possible energy shortage has led to increasing interest in technologies for generation of renewable electrical energy. Among various renewable energy sources, wind generation has been the leading source in the power industry.

During the last decade, the concept of the variable-speed wind turbine (VSWT) equipped with a doubly fed induction generator (DFIG) has received increasing attention due to its noticeable advantages over other wind turbine (WT) concepts [1]-[4]. In the DFIG concept, the induction generator (IG) is grid-connected at the stator terminals, but the rotor terminals are connected to the grid via a partial-load variable frequency AC/DC/AC converter (VFC) and a transformer. The VFC only needs to handle a fraction (25-30%) of the total power to achieve full control of the generator. Compared to the fixed-speed wind turbine with IG, the VSWT with DFIG can provide decoupled control of active and reactive power of the generator, more efficient energy production, improved

power quality, and improved dynamic performance during power system disturbances such as network voltage sags and short circuits. Compared to the VSWT equipped with a synchronous generator (SG), in which a full load VFC is connected directly between the generator stator and the grid, the VFC of the DFIG is smaller in size and therefore much cheaper.

On the other hand, the VFC and its power electronics (IGBT-switches) are the most sensitive part of this wind turbine generator system (WTGS) when subjected to transient disturbances in the power network. As a result of such disturbances, the rotor-side converter (RSC) of the VFC might be blocked (it stops switching and trips) due to the protection from over-current in the rotor circuit and the WT might be tripped from the system.

The behavior of the VFC and the associated WTGS relies on the performance of its control system. With well-designed controllers, it is possible to increase the chance of the WTGS to remain in service during grid disturbances. In the last decade, various modern control techniques such as adaptive control, variable structure control and intelligent control [5]-[7], have been intensively studied for controlling the nonlinear components in power systems. However, these control techniques have few real applications probably due to their complicated structures or the lack of confidence in their stability. Therefore, the conventional PI controllers, because of their simple structures, are still the most commonly used control techniques in power systems, as can be seen in the control of the WTs equipped with DFIGs [4], [8]-[10]. Unfortunately, tuning the PI controllers is tedious and it might be difficult to tune the PI gains properly due to the nonlinearity and the high complexity of the system. Over the years, heuristic search based algorithms such as genetic algorithms (GAs), tabu search algorithm and simulated annealing (SA) have been used for power system stabilizers (PSS) design [11]-[13]. However, when the parameters being optimized are highly correlated, the performance of these heuristic search algorithms degrades [14].

Recently, a new technique based on swarm intelligence called particle swarm optimization (PSO) has been successfully used for single- and multi-objective nonlinear optimization [15]-[18]. The use of PSO for designing a single PID controller in the automatic voltage regulator (AVR) system of a conventional turbo generator has been reported in [19]. However, this design is based on the step response and did not investigate the transient performance of the controller.

In this paper, the PSO algorithm is used to find the optimal parameters of the various PI controllers for the rotor-side converter of the VFC. A new time-domain fitness function is defined to measure the performance of the controllers. Simulation results show that the proposed design approach is efficient to find the optimal parameters of the PI controllers and therefore improves the transient performance of the WTGS over a wide range of operating conditions.

II. WIND FARM AND POWER NETWORK MODEL

Figure 1 shows the single-line diagram of a large wind farm (WF) connected to a power network. The WF is represented by an aggregated model in which hundreds of individual WTs and DFIGs are modeled as one equivalent DFIG driven by a single equivalent WT [1]. The WF is connected to the power network through a step-up transformer and two parallel lines. A three-phase balanced electric load at the sending end bus is modeled as a constant impedance load. The system is simulated in the PSCAD/EMTDC environment. The parameters of the system components are given in the Appendix.
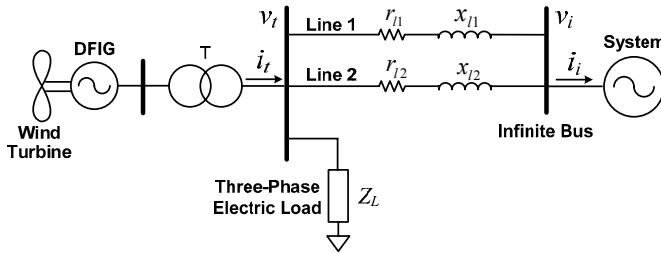

Fig. 1. Single-line diagram of a wind farm connected to a power network

III. MODELING AND CONTROL OF DFIG

The basic configuration of a DFIG driven by a WT is shown in Fig. 2. The wound-rotor induction machine in this configuration is fed from both stator and rotor sides. The stator is directly connected to the grid while the rotor is fed through a VFC. In order to produce electrical power at constant voltage and frequency to the utility grid over a wide operation range from subsynchronous to supersynchronous speed, the power flow between the rotor circuit and the grid must be controlled both in magnitude and in direction. Therefore, the VFC consists of two four-quadrant IGBT PWM converters connected back-to-back by a dc-link capacitor [8]. The crow-bar is used to short-circuit the RSC in order to protect the RSC from over-current in the rotor circuit during grid faults.

Control of the VFC includes the RSC control [4], [8]-[10] and the grid-side converter (GSC) control [8]. The objective of the RSC is to govern both the stator-side active and reactive powers independently. Figure 3 shows the overall vector control scheme of the RSC. In order to achieve independent control of the stator active power P_s (by means of speed control) and reactive power Q_s by means of rotor current regulation, the instantaneous three-phase rotor currents i_{rabc} are sampled and transformed to d-q components i_{dr} and i_{qr} in the stator-flux oriented reference frame.

Subsequently, Q_s and P_s (thus the generator rotor speed ω_r) can be represented as functions of the individual current components. Therefore, the reference values of i_{dr} and i_{qr} can be determined directly from the Q_s and ω_r commands. The actual d-q current signals (i_{dr} and i_{qr}) are then compared with their reference signals (i_{dr}^* and i_{qr}^*) to generate the error signals, which are passed through two PI controllers to form the voltage signals v_{dr1} and v_{qr1}. The two voltage signals (v_{dr1} and v_{qr1}) are compensated by the corresponding cross coupling terms (v_{dr2} and v_{qr2}) to form the d-q voltage signals v_{dr} and v_{qr}. They are then used by the PWM module to generate the IGBT gate control signals to drive the IGBT converter.
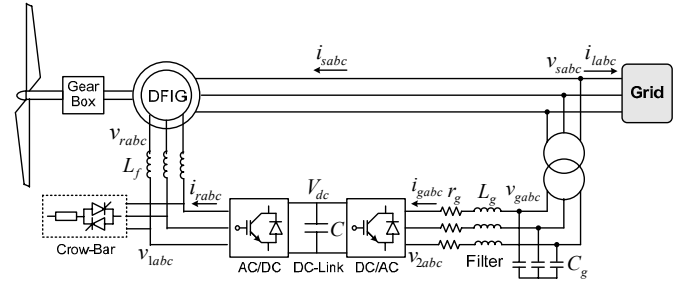

Fig. 2. Configuration of a DFIG driven by a wind turbine.

The objective of the GSC is to keep the dc-link voltage constant regardless of the magnitude and direction of the rotor power [8]. In this paper, the GSC control scheme is also designed to regulate the reactive power. This might be necessary to keep the voltage within the desired range, when the DFIG feeds into a weak power system without any local reactive compensation. When the DFIG feeds into a strong power system, the reactive power command of Q_g can be simply set to zero. Figure 4 shows the overall control scheme of the GSC. The actual signals of the dc-link voltage and the reactive power (V_{dc} and Q_g) are compared with their commands (V_{dc}^* and Q_g^*) to form the error signals, which are passed through the PI controllers to generate the reference signals for the d-axis and q-axis current components (i_{dg}^* and i_{qg}^*), respectively. The instantaneous ac-side three-phase current of the GSC are sampled and transformed into d-axis and q-axis current components i_{dg} and i_{qg} by applying the synchronously rotating reference frame transformation. The actual signals (i_{dg} and i_{qg}) are then compared with the corresponding reference signals to form the error signals, which are passed through two PI controllers. The voltage signals (v_{dg1} and v_{qg1}) are compensated by the corresponding cross coupling terms to form the d-q voltage signals v_{dg} and v_{qg}. They are then used by the PWM module to generate the IGBT gate control signals to drive the IGBT converter.

IV. PARTICLE SWARM OPTIMIZATION

Particle swarm optimization is inspired by the paradigm of birds flocking. It searches for the optimal solution from a population of moving particles. Each particle represents a potential solution and has a position in the problem space represented by a position vector x_i. A swarm of particles moves through the problem space, with the moving velocity
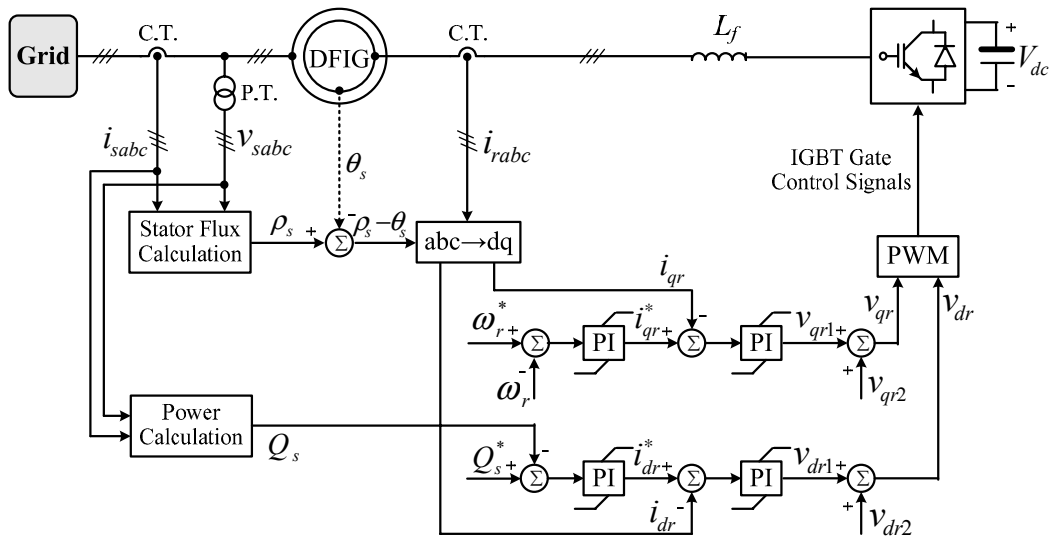
Fig. 3. Overall vector control scheme of the rotor-side converter: $v_{qr2} = s\omega_s(\sigma L_r i_{dr} + L_m^2 i_{ms} / L_s)$, $v_{dr2} = -s\omega_s \sigma L_r i_{qr}$, $\sigma = 1 - L_m^2 /(L_s L_r)$.
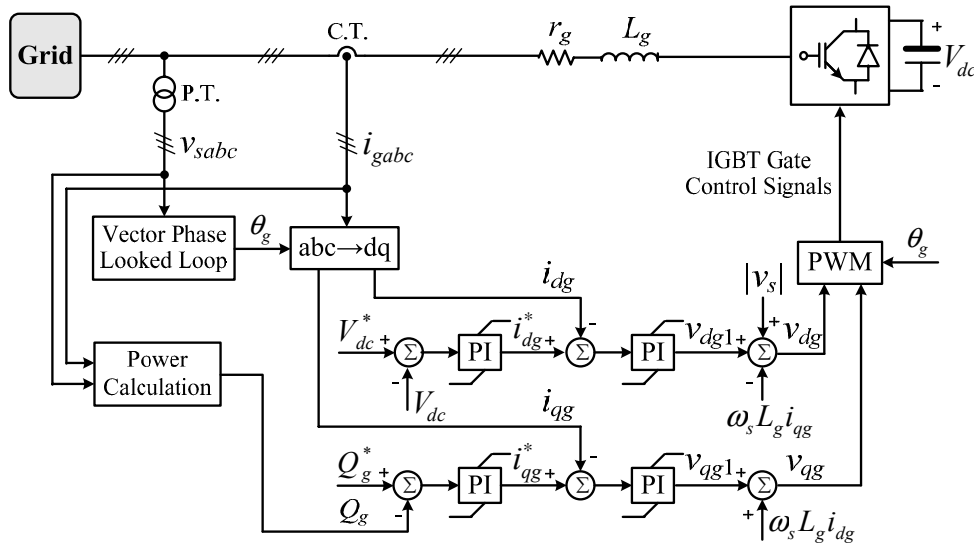

Fig. 4. Overall control scheme of the grid-side converter.

of each particle represented by a velocity vector v_i. At each time step, a fitness function f representing a quality measure is calculated by using x_i as input. Each particle keeps track of its individual best position $x_{i,pbest}$, which is associated with the best fitness it has achieved so far. Furthermore, the best position among all the particles obtained so far in the swarm is kept track of as x_{gbest}. This information is shared by all particles. The PSO algorithm is implemented in the following iterative procedure to search for the optimal solution.

(i) Initialize a population of particles with random positions and velocities of M dimensions in the problem space.

(ii) Define a fitness measure function to evaluate the performance of each particle.

(iii) Compare each particle's present position x_i with its $x_{i,pbest}$ based on the fitness evaluation. If the current position x_i is better than $x_{i,pbest}$, then set $x_{i,pbest} = x_i$.

(iv) If $x_{i,pbest}$ is updated, then compare each particle's $x_{i,pbest}$ with the swarm best position x_{gbest} based on the fitness evaluation. If $x_{i,pbest}$ is better than x_{gbest}, then set $x_{gbest} = x_{i,pbest}$.

(v) At iteration k, a new velocity for each particle is updated by

$$v_i(k+1) = w \cdot v_i(k) + c_1 \phi_1(x_{i,pbest}(k)-x_i(k))$$
$$+ c_2 \phi_2(x_{gbest}(k)-x_i(k)) \qquad i = 1, 2, \cdots, N \qquad (1)$$

(vi) Based on the updated velocity, each particle then changes its position according to the following equation.

$$x_i(k+1) = x_i(k) + v_i(k+1) \qquad i = 1, 2, \cdots, N \qquad (2)$$

(vii) Repeat steps (iii)-(vi) until a criterion, usually a sufficiently good fitness or a maximum number of iterations is achieved. The final value of x_{gbest} is regarded as the optimal solution of the problem.

In (1), c_1 and c_2 are positive constants representing the weighting of the acceleration terms that guide each particle toward the *individual best* and the *swarm best* positions $x_{i,pbest}$ and x_{gbest}, respectively; ϕ_1 and ϕ_2 are uniformly distributed random numbers in [0, 1]; w is a positive inertia weight developed to provide better control between exploration and exploitation; N is the number of particles in the swarm. The velocity v_i is limited to the range [$-v_{max}$, v_{max}]. If the velocity violates this limit, it is set to the relevant upper- or low-bound value. The last two terms in (1) enable each particle to perform a local search around its individual best position $x_{i,pbest}$ and the swarm best position x_{gbest}. The first term in (1) enables each particle to perform a global search by exploring a new search space.

The multi-agent (particles) searching and information sharing mechanism in PSO enable a fast and efficient search for the optimal solution. In many cases, the PSO algorithm yields superior performance to other evolutionary computation algorithms, such as genetic algorithms.

V. DESIGN OF OPTIMAL PI CONTROLLERS

In the WTGS equipped with the DFIG, the VFC and its power electronics (IGBT-switches) are the most sensitive part. The converter action will probably determine the operation of the WTGS during transient disturbances in the power grid. Grid faults, for example, even far away from the location of the WF, can cause voltage sags at the connection point of the WT. This voltage sag will result in an imbalance between the turbine input power and the generator output power and therefore a high current in the stator windings of the DFIG. Because of the magnetic coupling between stator and rotor, this current will also flow in the rotor circuit and the converter. Since the power rating of the IGBT converter is only 25-30% of the induction generator power rating, this over-current can lead to the destruction of the converter. On the other hand, the behavior of the converter also depends on the control system. If the controllers are tuned properly, it is possible to limit the rotor current and therefore improve the converter's (especially the RSC's) performance during the transient disturbances [20]. However, tuning controllers is tedious and it is difficult to achieve a set of optimal parameters manually. In this section, the PSO algorithm is applied to find the optimal parameters of the RSC controllers automatically.

In the RSC control loops (Fig. 3), there are four PI controllers and each of them has a proportional gain and an integral time constant. The objective of the PSO is to find the optimal parameters of the four PI controllers, namely, four proportional gains (K_{ω}, K_Q, K_d, and K_q) and four integral time constants (T_{ω}, T_Q, T_d, and T_q), to optimize some performance measure function (fitness function). Generally, the PI controller performance in the time domain can be measured by a set of parameters: the overshoot M_p, the rise time t_r, the settling time t_s, and the steady-state error E_{ss}. In

this paper, the objective is to reduce the over-current in the rotor circuit during grid faults. Therefore, a new performance measure function is defined as follows:

$$f(x) = \beta \cdot \Delta I_{r,max} + (1-\beta)(t_s-t_0) + \alpha \cdot |E_{ss}| \qquad (3)$$

where $x = [K_{\omega}, K_Q, K_d, K_q, T_{\omega}, T_Q, T_d, T_q]$ represents the position vector of each particle; β and α are weighting factors; $\Delta I_{r,max}$ is the maximum rotor current magnitude deviation of the DFIG; t_0 is the starting time of the disturbance; and t_s is the settling time.

The weighting factors β and α in the performance measure function $f(x)$ are used to satisfy different design requirements. If a large value of β is used, then the objective is to reduce the over-current in the rotor circuit. If a small value of β is used, then the objective is to reduce the settling time. The weighting factor α is introduced to minimize the steady-state error.

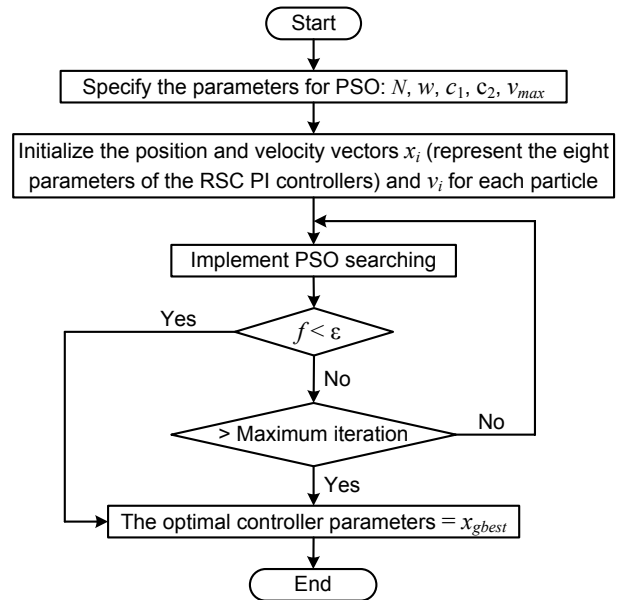The overall design procedure is shown as the flowchart in Fig. 5.

Fig. 5. Flowchart of the optimal PI controller parameters design procedure

VI. SIMULATION RESULTS

The PI controllers in Figs. 3 and 4 are initially designed (but not optimal) at a specific operating point, where the WTGS in Fig. 1 is operated at a supersynchronous speed with the slip frequency around -0.2 pu, an output active power of 0.75 pu, an output reactive power of 0.125 pu (the RSC reactive power command is set to 0.125 pu while the GSC reactive power command is set to 0) and a rotor current magnitude of 11.0 kA. The parameters of the RSC controllers are then optimized at this operating point using the PSO algorithm. Five particles are used in the simulation and the position vector of the first particle is initialized as the initially designed parameters; while the position vectors of the other four particles are initialized with the values around the initially designed parameters using (1). The values of c_1 and c_2 in (1) are chosen as 2; the inertia constant $w = 0.8$. The weighting factors in (3) are chosen as $\alpha = 0$, $\beta =$

1 in order to limit the over-current in the rotor circuit during grid faults. The PSO is implemented with 30 trial runs by applying a 100 ms three-phase short circuit at the receiving end of line 2. The initial values and the optimal values found by the PSO for the RSC controller parameters are given in Table I.

TABLE I
INITIAL AND OPTIMAL PARAMETERS OF THE RSC CONTROLLERS

	K_ω	K_Q	K_d	K_q	T_ω	T_Q	T_d	T_q
Initial design	8.48	0.01	2.89	1.79	0.081	2.0	0.028	0.065
Optimal design	18.23	0.001	3.05	4.87	0.038	1.0	0.056	0.21

A. Case Study I: A Three-Phase Short Circuit Test at Receiving End of Line 2

A 100 ms temporary three-phase short circuit is applied to the receiving end of line 2 at $t = 5.0$ sec. Figure 6 shows the magnitudes of the DFIG rotor current for both designs. The rotor current magnitude is limited to 14 kA when applying the optimal design, which is much smaller than that of 19 kA when using the initial design. The reduction of the over-current in the rotor circuit avoids the blocking of the RSC and therefore achieves continuous operation of the WTGS during this grid fault. Due to the stator flux oscillations during the transient state after the grid fault, the rotor current oscillates with a frequency near the synchronous frequency [1], as can be seen in Fig. 6.
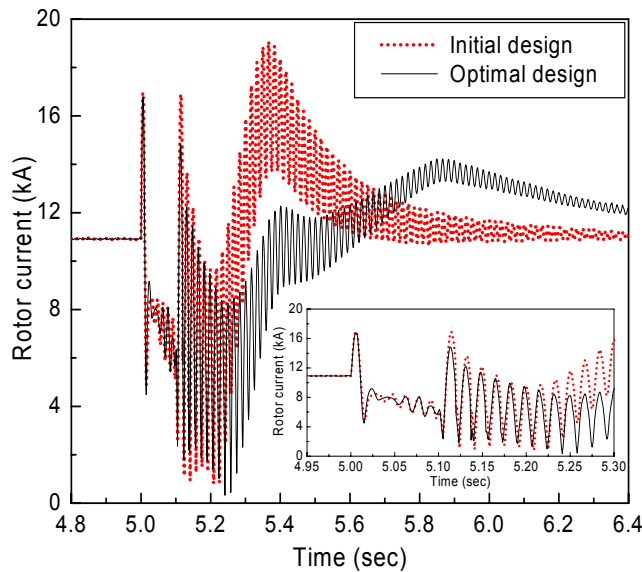

Fig. 6. Comparison of the initial design and the optimal design in Case I: DFIG rotor current

The cost of reducing the over-current in the rotor circuit is an increase of the settling time (Fig. 6) and the larger oscillations of the dc-link voltage (Fig. 7). However, the settling time is irrelevant to the design objective and therefore is not considered in this paper (by choosing $\beta = 1$ in (3)). Moreover, the largest oscillating magnitudes of the dc-link voltage for both designs, which occur in the first swing after the fault, are close and within the limits of the dc-link voltage deviations. Therefore, the dc-link voltage oscillations in both designs do not affect the continuous operation of the WTGS.
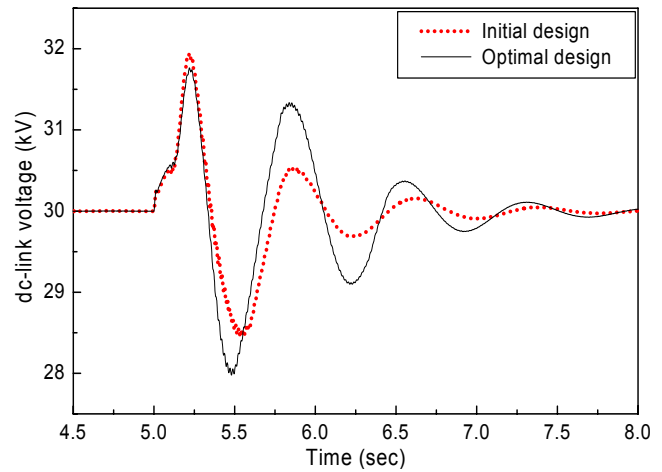

Fig. 7. Comparison of the initial design and the optimal design in Case I: VFC dc-link voltage

B. Case Study II: A Three-Phase Short Circuit Test at Sending End of Line 2

The two designs are compared for another case, in which a three-phase short circuit is applied to the sending end of line 2 and 100ms thereafter line 2 is tripped off from the system. In this case, the system in Fig. 1 operates at a new operating point after the fault is cleared. Figure 8 compares the magnitudes of the DFIG rotor current for both designs. Again, the magnitude of the post-fault rotor current is limited to 13.5 kA when applying the optimal design, which is much smaller than that of 24 kA when applying the initial design. It is concluded that the optimal design reduces the over-current in the rotor circuit effectively over a wide range of operating conditions.
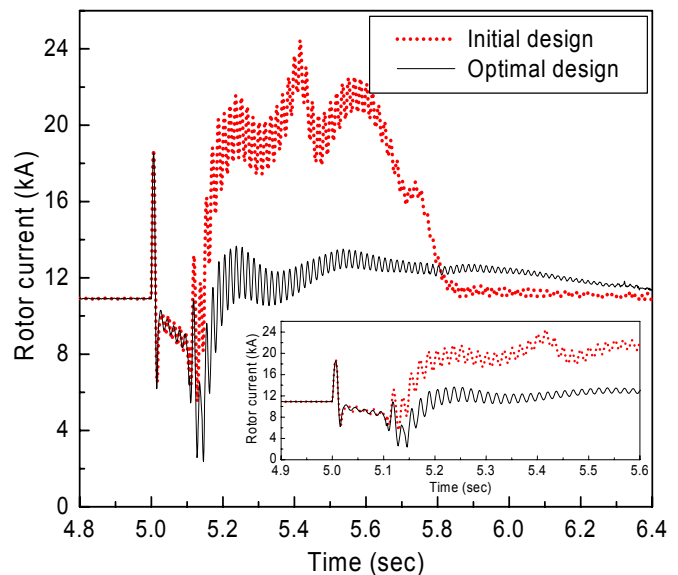

Fig. 8. Comparison of the initial design and the optimal design in Case II: DFIG rotor current

As in Case I, the oscillations of the dc-link voltage, when applying the optimal design, are slightly larger than when applying the initial design, as shown in Fig. 9.
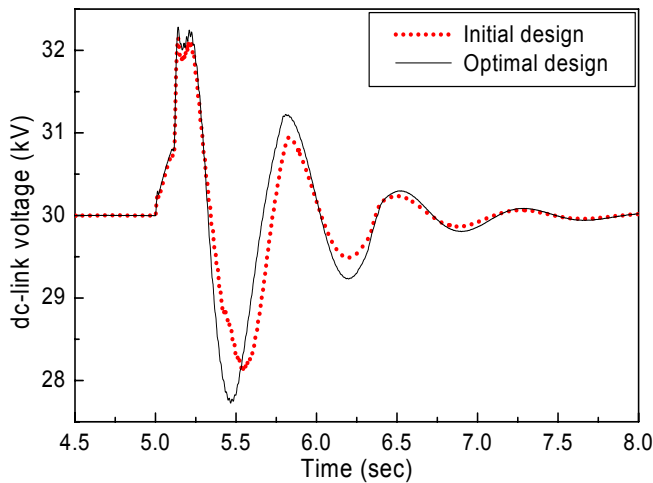

Fig. 9. Comparison of the initial design and the optimal design in Case II: VFC dc-link voltage

VII. CONCLUSION

An equivalent doubly fed induction generator (DFIG) driven by a wind turbine has been modeled to represent an aggregated model of a large wind farm which is connected to a power network. The control system of the DFIG consists of the control of two back-to-back connected IGBT PWM converters, namely, the rotor-side converter (RSC) and the grid-side converter (GSC). The linear PI controllers are used to control both converters and their parameters are initially designed at a specific operating point.

The particle swarm optimization (PSO) algorithm is then used to find the optimal parameters of the PI controllers for the RSC in order to minimize the over-current in the rotor circuit during grid faults. A new time-domain fitness function is defined to measure the performance of the controllers. Simulation studies are carried out at the operating point where the optimal controllers are designed, as well as at another operating point where the optimal controllers have not been designed. Results show that the proposed design approach is efficient to find the optimal parameters of the PI controllers and improves the transient performance of the wind turbine generator system over a wide range of operating conditions.

APPENDIX

Wind turbine: rated capacity = 400 MW, cut-in wind speed = 3.5 m/s, cut-out wind speed = 27 m/s, rated wind speed = 14 m/s, number of blades = 3, rotor diameter = 104 m, swept area = 8495 m^2, rotor speed (variable) = 8.5-15.3 rpm.

Induction generator (on a 400 MW base): rated power = 400 MW, rated stator voltage = 22 kV, r_s = 0.0079 pu, r_r = 0.025 pu, L_{ls} = 0.07937 pu, L_{lr} = 0.40 pu, L_m = 4.4 pu.

Power network (on 400 MVA, 230 kV bases): $r_{l1} = r_{l2}$ = 0.02 pu, $x_{l1} = x_{l2}$ = 0.4 pu, constant impedance load Z_L = 4.5 + j2.18 pu, transformer turn ratio: 22kV/230kV.

REFERENCES

[1] V. Akhmatov, Analysis of Dynamic Behavior of Electric Power Systems with Large Amount of Wind Power, Ph.D. thesis, Technical University of Denmark, Kgs. Lyngby, Denmark, Apr. 2003.

[2] R. Datta and V. T. Ranganathan, "Variable-speed wind power generation using doubly fed wound rotor induction – a comparison with alternative schemes,' *IEEE Trans. Energy Conversion*, vol. 17, no. 3, Sept. 2002, pp. 414-421.

[3] M. V. A. Nunes, J. A. Pecas Lopes, H. H. Zurn, U. H. Bezerra, and R. G. Almeida, "Influence of the variable-speed wind generators in transient stability margin of the conventional generators integrated in electrical grids," *IEEE Trans. Energy Conversion*, vol. 19, no. 4, Dec. 2004, pp. 692-701.

[4] J. Morren and S. W. H. de Haan, "Ridethrough of wind turbines with doubly-fed induction generator during voltage dip," *IEEE Trans. Energy Conversion*, vol. 20, no. 2, Jun. 2005, pp. 435-441.

[5] M. Lown, E. Swidenbank, B. W. Hogg, "Adaptive fuzzy logic control of a turbine generator system," *IEEE Trans. Energy Conversion*, vol. 12, no. 4, Dec. 1997, pp. 394-399.

[6] Y.-Y. Hsu, C.-H. Cheng, "Variable structure and adaptive control of a synchronous generator," *IEEE Trans. Aerospace and Electronic Systems*, vol. 24, no. 4, July 1988, pp. 337-345.

[7] G. K. Venayagamoorthy, R. G. Harley, and D. C. Wunsch, "Comparison of heuristic dynamic programming and dual heuristic programming adaptive critics for neurocontrol of a turbogenerator," *IEEE Trans. Neural Networks*, vol. 13, no. 3, May 2002, pp. 764-773.

[8] R. Pena, J. C. Clare, and G. M. Asher, "Doubly fed induction generator using back-to-back PWM converters and its application to variable-speed wind-energy generation," *IEE Proceedings – Electric Power Applications*, vol. 143, no. 3, May 1996, pp. 231-241.

[9] A. Tapia, G. Tapia, J. X. Ostolaza, and J. R. Saenz, "Modeling and control of a wind turbine driven doubly fed induction generator," *IEEE Trans. Energy Conversion*, vol. 18, no. 2, Jun. 2003, pp. 194-204.

[10] T. Tang and L. Xu, "A flexible active reactive power control strategy for a variable speed constant frequency generating system," *IEEE Trans. Power Electronics*, vol. 10, no. 4, Jul. 1995, pp. 472-477.

[11] Y. L. Abdel-Magid, M. A. Abido, S. Al-Baiyat, and A. H. Mantawy, "Simultaneous stabilization of multimachine power systems via genetic algorithms," *IEEE Trans. Power Systems*, vol. 14, no. 4, Nov. 1999, pp. 1428-1439.

[12] M. A. Abido, "A novel approach to conventional power system stabilizer design using tabu search," *Int. Journal Electrical Power and Energy Systems*, vol. 21, no. 6, Aug. 1999, pp. 443-454.

[13] M. A. Abido, "Robust design of multimachine power system stabilizers using simulated annealing," *IEEE Trans. Energy Conversion*, vol. 15, no. 3, Sept. 2000, pp. 297-304.

[14] D. B. Fogel, Evolutionary Computation: Toward a New Philosophy of Machine Intelligence, New York: IEEE Press, 2000, ISBN 0-7803-5379-X.

[15] J. Kennedy and R. C. Eberhart, "Particle swarm optimization," in *Proc. of IEEE International Conference on Neural Networks*, Piscataway, NJ, USA, Nov. 27-Dec. 1, 1995, vol. 4, pp. 1942-1948.

[16] Y. Shi and R. C. Eberhart, "A modified particle swarm optimizer," in *Proc. of IEEE International Conference on Evolutionary Computation*, Piscataway, NJ, USA, May 4-9, 1998, pp. 69-73.

[17] M. Clerc and J. Kennedy, "The particle swarm – explosion, stability, and convergence in a multidimensional complex space," *IEEE Trans. Evolutionary Computation*, vol. 6, no. 1, pp. 58-73, Feb. 2002.

[18] J. Kennedy and R. C. Eberhart, *Swarm Intelligence*. San Mateo, CA: Morgan Kaufmann, 2001.

[19] Z.-L. Gaing, "A particle swarm optimization approach for optimum design of PID controller in AVR system," *IEEE Trans. Energy Conversion*, vol. 19, no. 2, June 2004, pp. 384-391.

[20] J. B. Ekanayake, L. Holdsworth, X. G. Wu, and N. Jenkins, "Dynamic modeling of doubly fed induction generator wind turbines," *IEEE Trans. Power Systems*, vol. 18, no. 2, May 2003, pp. 803-809.